lockjaw encodes a zebrafish *tfap2a* required for early neural crest development

Robert D. Knight[1], Sreelaja Nair[1], Sarah S. Nelson[1], Ali Afshar[1], Yashar Javidan[1], Robert Geisler[2], Gerd-Joerg Rauch[2] and Thomas F. Schilling[1,*]

[1]Department of Developmental and Cell Biology, University of California, Irvine, CA 92697, USA
[2]Max-Planck-Institut für Entwicklungsbiologie, Spemannstrasse 35, 72076, Tübingen, Germany
*Author for correspondence (e-mail: tschilli@uci.edu)

Accepted 1 May 2003

Development 130, 5755-5768

doi:10.1242/dev.00575

Summary

The neural crest is a uniquely vertebrate cell type that gives rise to much of the craniofacial skeleton, pigment cells and peripheral nervous system, yet its specification and diversification during embryogenesis are poorly understood. Zebrafish homozygous for the *lockjaw* (*low*) mutation show defects in all of these derivatives and we show that *low* (allelic with *montblanc*) encodes a zebrafish *tfap2a*, one of a small family of transcription factors implicated in epidermal and neural crest development. A point mutation in *low* truncates the DNA binding and dimerization domains of *tfap2a*, causing a loss of function. Consistent with this, injection of antisense morpholino oligonucleotides directed against splice sites in *tfap2a* into wild-type embryos produces a phenotype identical to *low*. Analysis of early ectodermal markers revealed that neural crest specification and migration are disrupted in *low* mutant embryos. TUNEL labeling of dying cells in mutants revealed a transient period of apoptosis in crest cells prior to and during their migration. In the cranial neural crest, gene expression in the mandibular arch is unaffected in *low* mutants, in contrast to the hyoid arch, which shows severe reductions in *dlx2* and *hoxa2* expression. Mosaic analysis, using cell transplantation, demonstrated that neural crest defects in *low* are cell autonomous and secondarily cause disruptions in surrounding mesoderm. These studies demonstrate that *low* is required for early steps in neural crest development and suggest that *tfap2a* is essential for the survival of a subset of neural crest derivatives.

Key words: *Danio rerio*, Craniofacial, Pigment, Apoptosis, Montblanc, *AP2*, Hox

Introduction

The vertebrate neural crest forms the pigmentation of the body, peripheral innervation, and much of the cartilage and bone of the skull. Disruption of neural crest development in humans results in neuropathies, aberrant pigmentation and craniofacial defects (Schilling, 1997; Maschhoff and Baldwin, 2000; Epstein, 2001; Manie et al., 2001). Molecular mechanisms that control the differentiation of many of these derivatives have been studied extensively, but less is known about the early events that induce neural crest cells and specify their fates. Neural crest cells are induced at the lateral edges of the neural plate during neurulation, lose adhesion with the neuroepithelium and migrate along defined pathways (LeDouarin, 1982; Christiansen et al., 2000). These early crest cells are thought to be multipotent, and only later acquire their fates from their migratory environments, but a growing body of evidence suggests that many crest cells may be specified much earlier.

Two secreted signals have been suggested to induce neural crest during gastrulation, bone morphogenetic proteins (Bmps) and Wnts (Nieto, 2001; Aybar and Mayor, 2002). One key step is thought to be attenuation of Bmp signaling in the neural plate by specific antagonists (Chordin, Noggin) and posteriorizing signals (Wnt, Fgf and Retinoic acid) from adjacent mesoderm. Recent evidence has also supported the role of Wnt expressed in the adjacent ectoderm as a neural crest inducer (Garcia-Castro et al., 2002), and Delta/Notch signaling in the specification of trunk neural crest (Cornell and Eisen, 2000; Cornell and Eisen, 2002; Endo et al., 2002). Following its induction, the location of a neural crest cell in the ectoderm prior to migration then plays a crucial role in determining its segment and cell-type specific fates. Cranial neural crest cells that will migrate into the pharyngeal arches are organized along the anteroposterior axis into regions fated to form each arch segment (Lumsden et al., 1991; Schilling and Kimmel, 1994; Kontges and Lumsden, 1996). In zebrafish, the position within the mediolateral (ML) axis of the premigratory neural crest also determines if a cell will adopt a pigment cell fate over a neural or glial fate (Schilling and Kimmel, 1994; Kelsh and Raible, 2002). Wnt signals arising from the dorsal midline of the ectoderm bias this choice of cell type; activation of Wnt signaling promotes pigment cell fates (Dorsky et al., 1998). Thus, the same signals that induce neural crest cells may also specify their future migration patterns and fates within the embryo.

In addition to signaling molecules, a growing list of transcription factors appear to function in the early premigratory crest. These include the related zinc-finger genes

snail, *slug* (Nieto et al., 1994; Sefton et al., 1998; del Barrio and Nieto, 2002) and *twist* (Soo et al., 2002), the forkhead transcription factor *foxd3* (Dottori et al., 2001; Kos et al., 2001; Sasai et al., 2001), Zic genes (Nakata et al., 1997; Nakata et al., 1998), and the paired transcription factor *pax3* (Epstein et al., 1991; Tassabehji et al., 1993). Another family of transcription factors implicated in early neural crest development is the Activator Protein 2 (AP2) family, defined by a unique, highly conserved DNA-binding domain (Hilger-Eversheim et al., 2000). There are at least four AP2 genes in mice (*Tcfap2a*, *Tcfap2b*, *Tcfap2g* and *Tcfap2d*), three of which are co-expressed in the early ectoderm and neural crest (Mitchell et al., 1991; Chazaud et al., 1996; Moser et al., 1995; Moser et al., 1997; Werling and Schorle, 2002). Mice mutant for AP2 family genes reveal important functions in development, for example *Tcfap2a* mutant mice have craniofacial, neural tube, body wall, limb and eye defects (Schorle et al., 1996; Zhang et al., 1996; Morriss-Kay, 1996). Chimaeric analyses using *Tcfap2a* mutant mice show that these five classes of defects are independent of one another, implicating *Tcfap2a* in multiple processes of development (Nottoli et al., 1998). The craniofacial defects in *Tcfap2a*$^{-/-}$ mice are correlated with extensive cell death in the cranial neural crest and neural tube. Neural crest derived pharyngeal cartilages and middle ear bones, as well as cardiac neural crest of the heart outflow tract are malformed and reduced (Brewer et al., 2002). However, two early cranial crest markers, *Pax3* and *Twist*, show no disruption in these mutant mice and neural crest migration appears to occur normally, as shown by combining a *Wnt1-lacZ* transgene with the *Tcfap2a*$^{-/-}$ mutation. This implicates *Tcfap2a* in the development of several neural crest populations, yet relatively little is known about the roles of *Tcfap2* at early stages of neural crest development.

We show that the craniofacial mutant *lockjaw* (*low*) disrupts a zebrafish *tfap2a* that is required for the formation of subsets of neural crest-derived cell types (subsets of sensory neurons, cartilages and pigment cells) and pharyngeal segments (second pharyngeal arch). Zebrafish *tfap2a* is expressed in the non-neural ectoderm during gastrulation and then is upregulated in premigratory neural crest. We find that *low* is required at these early stages for the survival of neural crest migrating from the hindbrain and spinal cord. This is reflected in disruption and loss of early gene expression in the neural crest, including that of *tfap2a* itself. We focus on the subpopulations of neural crest disrupted in *low* mutants and show that the requirement for *low* for neural crest cell survival is cell autonomous and segment specific. This is the first evidence for such segment and cell-type-restricted functions of *tfap2a* in neural crest.

Materials and methods

Animals and histology

Embryos were obtained in natural crosses and staged according to Kimmel et al. (Kimmel et al., 1995). The *low*^{ts213} mutation was identified in an ENU screen for abnormal jaw morphology (Schilling et al., 1996b), maintained in a Tubingen (Tu) background and heterozygotes were outcrossed to a reference (WIK) strain for mapping. Cartilages were stained with Alcian Blue, dissected and flat-mounted (Kimmel et al., 1998). To label aortic arches, fluorescent microspheres (Molecular Probes) were microinjected into the axial vein at 72 hours postfertilization (hpf) (0.1 μm diameter) (Isogai et al., 2001).

Mapping and cloning

The *low*^{ts213}mutation was mapped using bulked segregant analysis of F2 embryos and genome scanning with SSLPs (Geisler, 2002). A candidate gene for *low*^{ts213}, *tfap2a*, mapped within 6 cM of our map position for *low*^{ts213} as does the *montblanc* (*mob*^{m819}) mutation (W. Driever, personal communication). *tfap2a* was cloned from *low* mutants and wild-type siblings using primers designed against the published sequence (GenBank: AF457191). The fifth exon of *tfap2a* was amplified from genomic DNA preparations of individual *low* mutants and wild-type siblings using primers designed against flanking intron sequence (forward: CGCTCAGGTCTTATAAATAG-GC and reverse: CTGAGAGGTGGCTATTTCCCG). Restriction enzyme digest of PCR-amplified exon five by *Blp*I (New England Biolabs) was used to identify *low* mutants and heterozygotes from a panel of 192 mutant and wild-type siblings. Sequencing of DNA was performed using the BigDye Terminator Sequencing reagent on a thermal sequencer and reactions run on an ABI PRISM 310 sequencer (PE Applied Biosystems).

Ectopic expression and rescue experiments

PAC DNA clones (library obtained from C. Amemiya) containing *tfap2a* were identified by PCR directed to exon five (as above) and confirmed using Southern analysis (Amemiya et al., 1999). DNA purified for injection was diluted to a concentration of 1ug/μl and ~10 nl were injected into *low* mutants at the one- to two-cell stage (Fishman et al., 1997). Rescue was defined by the presence of small numbers of melanophores at 24 hpf, which are never seen in uninjected *low* mutant embryos.

Fate mapping and apoptosis assays

Wild-type and *low*^{ts213} mutant embryos were injected with 10 kDa DMNB-caged fluorescein (5 mg/ml). Fluorescein was then activated when embryos reached the eight-somite stage along the dorsal and lateral neural keel (David et al., 2002). Labeled cells were then inspected at 28 hpf either visually or by immunodetection of fluorescein. Apoptotic cell death was detected in whole embryos by terminal transferase dUTP nick-end labeling (TUNEL) using modifications suggested by the manufacturer (In Situ Cell Death Detection Kit; POD; Roche). Embryos were fixed for 3-4 hours at room temperature in 4% paraformaldehyde, permeabilized in acetone and blocked in 2% goat serum for 2-3 hours at room temperature.

Cell transplantation

Wild-type and mutant donor embryos were injected at the one- to two-cell stage with a mixture of 3% TRITC-dextran (neutral, 10,000 M_r) and 3% biotinylated-dextran (lysine-fixable, 10,000 M_r). At the three-somite stage, labeled premigratory neural crest cells were transplanted into *low* mutant hosts as described previously (Schilling et al., 1996a), into segment-specific locations according to the fate map (Schilling and Kimmel, 1994). Hindbrain cells are often co-transplanted with neural crest cells in these experiments, conveniently marking their segments of origin.

Morpholinos

Three different morpholino antisense oligonucleotides (translation start site of *tfap2a1*, ATGmo – ATTTCCAAAGCATTTTCATTG-GTTG; intron 3 splice donor junction; 3.1mo – GAAATTGCTTAC-CTTTTTTGATTAC; intron 5 splice acceptor junction, 5.1mo – CCTCCATTCTTAGATTTGGCCCTAT) were obtained from Gene Tools (Philomath, OR) and injected at the one- to two-cell stage. Efficacy of morpholinos directed against splice sites was evaluated using RT-PCR (Fig. 2F) with forward primers tfap2a-3f and tfap2a-4f designed to 464 bp and 777 bp of *tfap2a1* (GenBank Accession Number AF457191) (GGTCACGGCATTGATACTGG; CTGAGT-

GCCTGAACGCTTCC) in conjunction with reverse primer tfap2a-3r designed to 1184 bp of *tfap2a1* (GTCAAACAGCTCTGAATCCC).

Whole-mount in situ hybridization and immunohistochemistry

In situ hybridization was carried out as described previously (Thisse et al., 1993). An antisense 2050 bp riboprobe for *tfap2a* (Furthauer et al., 1997) was generated using SP6 polymerase from RZPD clone: MPMGp609H2035Q8 (www.rzpd.de) following linearization by *Kpn*I. Probes and antibodies used were: *crestin* (Rubinstein et al., 2000; Luo et al., 2001), *dlx2* (Akimenko et al., 1994), *endrb* (Parichy et al., 2000b), *foxd3* (Odenthal and Nusslein-Volhard, 1998), *dct* (Kelsh et al., 2000), *fms* and *xdh* (Parichy et al., 2000a), *gch* (Pelletier et al., 2001), *mitfa* (Lister et al., 1999), *hoxa2* and *hoxb2* (Prince et al., 1998; Amores et al., 1998), *gsc* (Stachel et al., 1993), *sox9b* (Li et al., 2002), *isl1* (Inoue et al., 1994), *spa/kit* (Parichy et al., 1999), *sna2* (Thisse et al., 1995), anti-Hu, mjAb 16A11 (Marusich et al., 1994), and anti-TH (Guo et al., 1999).

Results

Pigmentation and craniofacial defects in *lockjaw* mutants

Zebrafish embryos homozygous for the recessive lethal *lockjaw* (*low*^{ts213}) allele have reduced body pigmentation and cartilages of the pharyngeal skeleton. In wild-type embryos, 40-50 melanocytes differentiate on each side of the head at 28 hpf, just anterior and posterior to the otic vesicles (Fig. 1A), but embryos homozygous for *low*^{ts213} lack most of these early melanocytes, while formation of the pigmented epithelium of the retina is unaffected (Fig. 1B). Older embryos and larvae can be identified by ~30% reduction in pigment cell number, small eyes and a ventrally protruding jaw (Fig. 1C). Cartilage differentiates in the jaw and pharyngeal arches of wild-type larvae at 72 hpf (Fig. 1D,F), but *low*^{ts213} mutant cartilages are severely reduced, particularly in the second or hyoid arch (Schilling et al., 1996b) (Fig. 1E,G). Alcian staining revealed that the dorsal hyosymplectic cartilage of the hyoid is consistently absent in *low*^{ts213} mutants, while the ventral ceratohyal is reduced (Fig. 1G). By contrast, the jaw or mandibular arch is much less affected in *low*^{ts213} mutants. Its dorsal element, the palatoquadrate, forms an ectopic contact with and fuses to the anterior basicranial commissure of the skull (Fig. 1G,I). By dissecting these cartilages free of other tissues we find that branchial cartilages are present in over 95% of *low* mutants though variably reduced (Fig. 1E), while severe hyoid defects occur in all cases. In addition, other pharyngeal cell types such as the aortic arches are also reduced in *low* mutants as revealed by injection of fluorescent microspheres into the bloodstream (Fig. 1J-L). These defects in pigment and pharyngeal arches suggest that *low* may be required in their common precursors in the neural crest.

The *low*^{ts213} mutation disrupts a zebrafish *tfap2a*

Bulked segregant analysis of an F2 mapping cross localized *low* to linkage group 24 (LG24) on a meiotic map between markers z23011 and z3399 (Fig. 2A). The transcription factor *tfap2a* maps between these markers and is expressed in neural crest (B. Thisse, S. Pflumio, M. Furthauer, B. Loppin, V. Heyer, A. Degrave, R. Woehl, A. Lux, T. Steffan, X. Q. Charbonnier and C. Thisse, Zebrafish Information Network, http://zfin.org, 2001), therefore we tested *tfap2a* as a candidate gene for *low*. The amino acid sequence shows high similarity to mouse

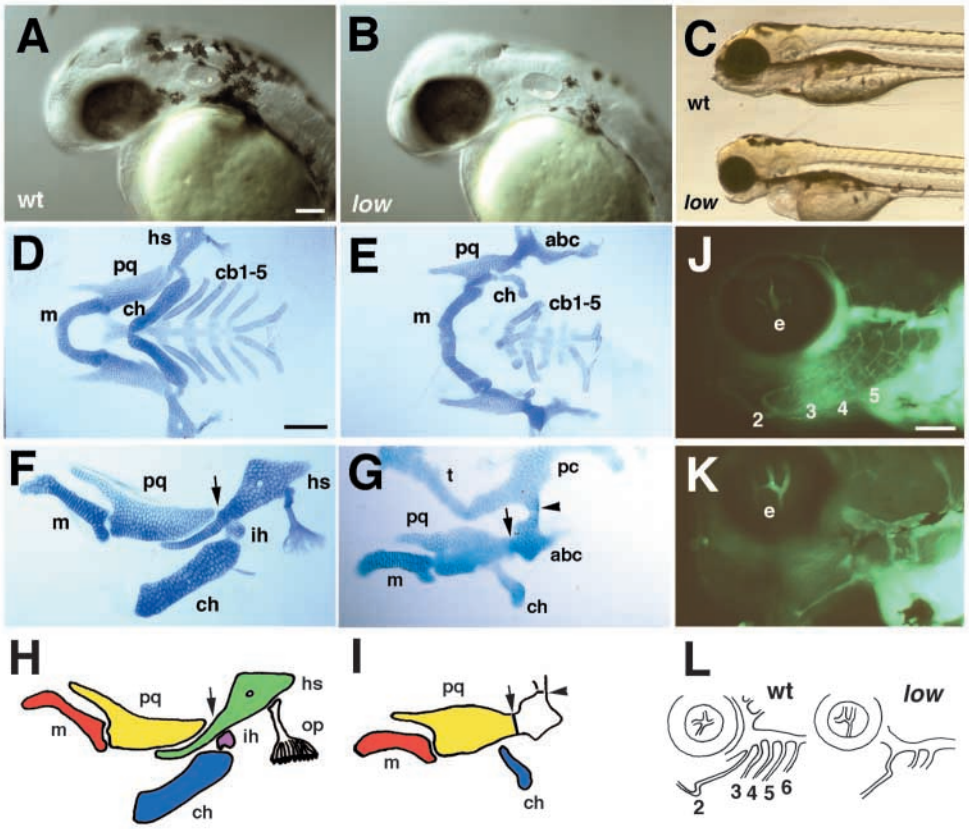

Fig. 1. Pigment, cartilage and aortic arch defects in *low*^{ts213} mutant zebrafish. Living wild-type and *low* mutant embryos. Lateral views (A-C) showing melanocyte reduction at 28 hpf (note normal eye pigmentation in *low*) and jaw defect at 72 hpf (C). (D-G) Dissected pharyngeal cartilages from 4 dpf wild-type (D,F) and *low* mutant (E,G) larvae, stained with Alcian Blue and shown in ventral (D,E) and lateral (F,G) view. (E,G) Branchial cartilages have been torn away. (H,I) Camera lucida drawings of mandibular and hyoid cartilages in wild type (F) and *low* mutant (G). Pharyngeal cartilages and joints (arrows) are absent or reduced in all but the mandibular arch in *low* mutants, which fuses with the anterior basicranial commissure of the skull. (J,K) Aortic arches in 4 dpf wild-type (J) and low mutant (K) larvae, labeled with fluorescent microspheres and shown in ventrolateral view. (L) Camera lucida drawings of aortic arches in wild-type (left) and defects in *low* mutants (right). abc, anterior basicranial commissure; cb1-5, ceratobranchials 1-5; ch, ceratohyal; e, eye; hs, hyosymplectic; ih, interhyal; m, Meckel's; op, opercular bone; pc, parachordals; pq, palatoquadrate; t, trabeculae. Scale bars: 100 μm.

Tcfap2a (68.5% overall identity, 98.3% identity within the DNA-binding and dimerization domains; data not shown). Further comparison of the corresponding genomic sequences revealed conservation of the exon-intron structure between the two species, indicating that this is a zebrafish orthologue of mouse *Tcfap2a*. Consequent sequence analysis of *tfap2a* in *low*^{ts213} mutant larvae revealed a point mutation of an adenosine (at 900 bp of the *tfap2a1* sequence) to a thymidine, creating a stop codon in place of a highly conserved lysine in the DNA-binding domain (Fig. 2B). This truncates the protein coding sequence and would result in deletion of the C terminus of the protein, including both the dimerization domain and most of the DNA-binding domain (Williams and Tijan, 1991; Garcia et al., 2000). This unique change also creates a

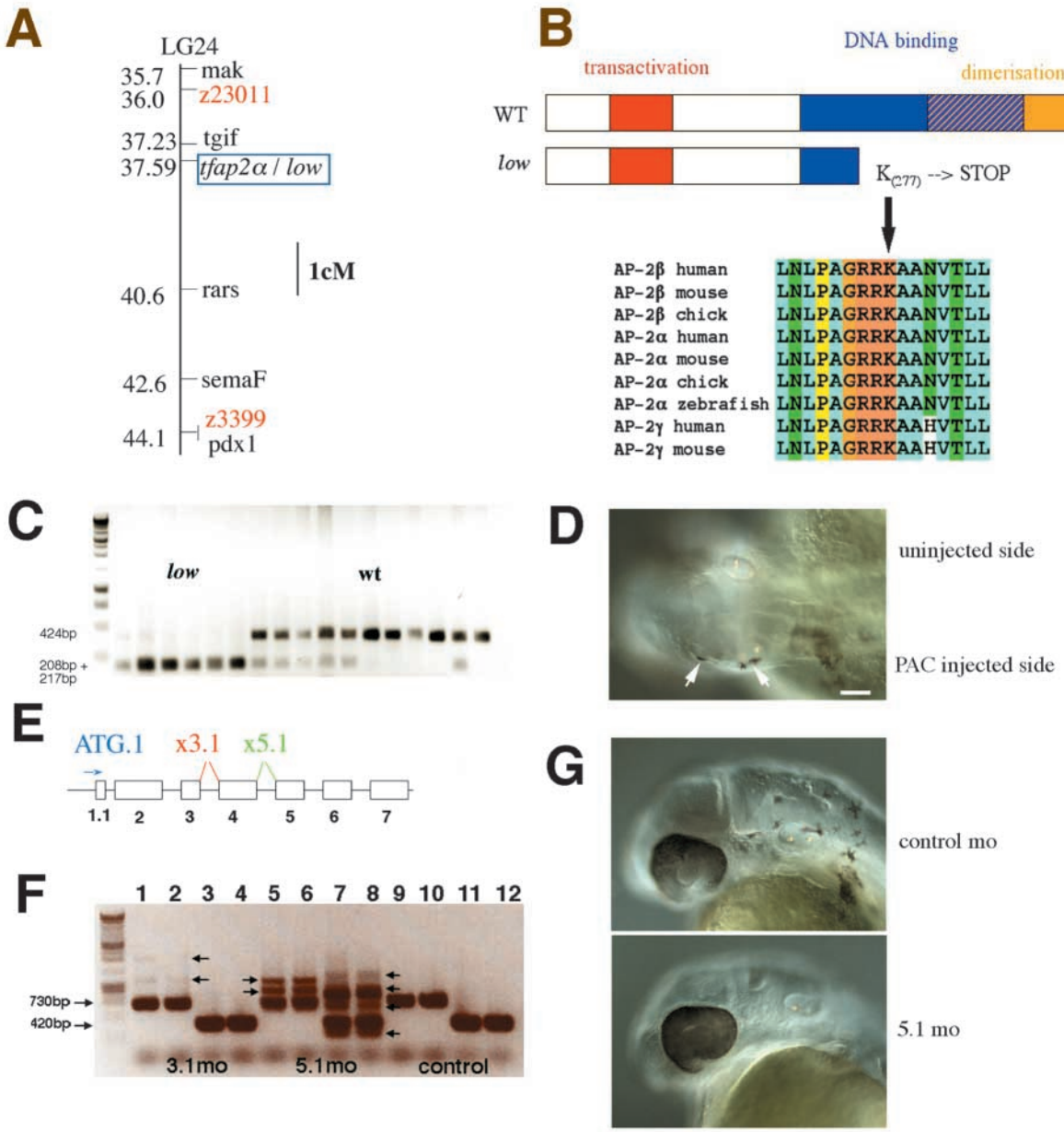

Fig. 2. *low*^{ts213} is a mutation in a zebrafish *tfap2a*. (A) The *tfap2a* gene is closely linked to the *low*^{ts213} locus. Both map to the long arm of linkage group 24 between SSCP markers z23011 and z3399. (B) *low*^{ts213} creates a stop codon in the conserved DNA-binding/dimerization domain of *tfap2a*, resulting in a truncated protein. (C) PCR products of 424 bp were amplified from exon 5 of tfap2a from preparations of individual 3 dpf *low* and sibling larvae. Digests by *Blp*I show co-segregation of the restriction site with the *low* phenotype producing bands of sizes 208 bp and 217 bp. (D) Unilateral rescue of melanophore development at 26 hpf by injection of a PAC containing *tfap2a* into one blastomere at the two-cell stage (arrows indicate rescued melanocytes). (E) Genomic organization of *tfap2a* and the locations of morpholino antisense oligonucleotides directed against splice acceptor sites. (F,G) Splicing defects in *tfap2a* transcripts following injection of splice-directed morpholinos. *tfap2a* was amplified from pools of 3.1mo (lanes 1-4) and 5.1mo (lanes 5-8) morpholino injected and control uninjected (lanes 9-12) animals using primers tfap2a-3f and tfap2a-3r directed to exons 3 and 7 (lanes 1,2,4-6,9,10) and primers tfap2a-4f and tfap2a-3r directed to exons 4 and 7 (lanes 3,4,7,8,11,12). Uninjected animals (lanes 9-12) showed PCR products of sizes 730 bp and 420 bp, in comparison with morpholino-injected animals in which additional PCR products were observed (black arrows) because of aberrant splicing (F). (G) These produce a phenotype similar to *low*^{ts213}. Scale bar: 100 μm.

restriction site for *Blp*I, allowing identification of *low* homozygotes by PCR amplification of exon5 (Fig. 2C). *Low* fails to complement *montblanc*^{m819} which is also a mutation in *tfap2a* and disrupts development of catecholaminergic neurons (Neuhauss et al., 1996) (W. Driever, personal communication)

As a direct demonstration that *tfap2a* is responsible for the *low* phenotype we performed rescue experiments. We took advantage of the consistent absence of melanophores in *low*^{ts213} mutant embryos between 24-27 hpf. Microinjection of 5-10 ng of a PAC (19:226) containing the *tfap2a* gene into embryos at the one- to two-cell stage, rescued local patches of melanophores in 28% (14/50) of *low* mutants, or in some cases gave unilateral rescue over large areas (Fig. 2D), while control PAC (D17:5) injections failed to do so (Fig. 2D).

To show further that reduction in *tfap2a* function causes the *low* phenotype, we injected one- to two-cell stage wild-type embryos with morpholino antisense oligonucleotides targeted to *tfap2a* (Fig. 2E-G). We first injected a morpholino directed against the putative translation start site of the *tfap2a1* splice form (ATGmo) but as much as 10 ng/embryo had no specific effect on neural crest derived pigment or cartilage. In zebrafish, there are multiple splice forms of *tfap2a*, with three alternative first exons as in mouse (Meier et al., 1995). Therefore, we tried morpholinos targeted to a splice donor site at the third exon (3.1mo) and to a splice acceptor site at the fifth exon (5.1mo), at positions 537 and 819 of the *tfap2a1* mRNA sequence, respectively (Fig. 2E). Five nanograms/embryo of the 5.1mo alone was sufficient to effectively phenocopy the pigment and jaw defects characteristic of *low* mutants (Fig. 2G; Table 1). This phenotype correlated with a dramatic change in *tfap2a* transcripts, in which regions of adjoining introns are not spliced correctly, as detected by RT-PCR using primers that amplify over these splice sites (Fig. 2F). Microinjection of the 3.1mo caused only a subtle delay in pigmentation when injected at 5 ng/embryo, but more effectively reduced pigmentation at 10-20 ng/embryo concentrations and this correlated with weaker affects on *tfap2a* RNA splicing (Fig. 2F). Notably, morpholino injections did not increase the severity of the phenotype when injected into homozygous *low*^{ts213} mutants, supporting the notion that *low*^{ts213} is a complete loss-of-function mutation.

tfap2a expression

Zebrafish *tfap2a* is first expressed at late blastula and early gastrula stages in a broad ventral domain of ectoderm (Fig. 3A,B), which corresponds to the non-neural ectoderm as revealed by comparison with *gata3* (Neave et al., 1995). By 80% epiboly, expression is upregulated in putative progenitors of the neural crest, and subsequently becomes restricted to two thin bands within the ectoderm, stretching from approximately the level of the prospective forebrain-midbrain junction to the posterior hindbrain initially and then progressively expanding posteriorly to spinal levels (Fig. 3C,D). Outside the ectoderm, *tfap2a* is also expressed in intermediate/lateral plate mesoderm (Fig. 3L). *tfap2a* expression in neural crest only partially overlaps the expression of *foxd3* and *sna2* at the six-somite stage, revealing early differences in gene expression within different populations of neural crest (data not shown).

By 24 hpf, *tfap2a* expression becomes confined predominantly to migrating neural crest and neurons within the central nervous system (CNS) (Fig. 3E). No expression can be detected in the epidermis at this stage. Expression in the pharyngeal arches is widespread throughout the neural crest-derived mesenchyme (Fig. 3F) and in small groups of cells migrating medial to each somite (data not shown). *tfap2a* is also expressed in neuronal groups within the telencephalon and ventral mesencephalon (Fig. 3G), as well as segmental groups of neurons within each rhombomere of the hindbrain (Fig. 3H). Prospective Rohon-Beard (RB) neurons within the spinal cord, which originate alongside neural crest, also express *tfap2a* at 24 hpf (Fig. 3I) (Cornell and Eisen, 2000).

To determine if expression of *tfap2a* mRNA was disrupted in *low* mutants we performed in situ hybridization at 12 and 24 hpf. Although in wild-type controls, dark labeling of *tfap2a*-expressing cells was achieved with coloration reactions lasting only a few hours, in *low* mutants incubation overnight gave very weak labeling (Fig. 3J,K). These results suggest either that the mutant mRNA is unstable and degraded after transcription or, alternatively, that *tfap2a* function is required for its own expression.

Table 1. Morpholinos effectively phenocopy the *low/tfap2* mutant

Genotype	Number of pigment defects/total number of defects (%)	Number of hyoid defects/total number of defects (%)
Wild type	0/120 (–)	0/85 (–)
lockjaw	73/75 (99%)	75/75 (100%)
Standard control (10 ng)	2/52 (4%)	0/52 (–)
tfap2α. ATG morpholino (10 ng)	0/68 (–)	0/68 (–)
tfap2α. 5′ morpholino (5 ng)	138/150 (92%)	70/75 (94%)
tfap2α. 3′ morpholino (5 ng)	26/56 (46%)	3/28 (11%)
tfap2α. 3′ morpholino (10 ng)	72/125 (58%)	21/62 (34%)

Defects in early neural crest specification in *low* mutants

To determine the stage at which neural crest development is disrupted in *low* mutants, we analyzed the expression of molecular markers of premigratory and migrating crest. Cranial neural crest is first visible morphologically at 10 hpf and becomes progressively more prominent posteriorly during somitogenesis. In six-somite stage wild-type embryos, the forkhead transcription factor *foxd3* is expressed throughout neural crest cells emerging from midbrain, hindbrain and anterior spinal regions, while *crestin* (*ctn*) is strongly expressed only in neural crest posterior to the otic vesicle (Fig. 4A,C,E). In *low* mutants, *ctn* expression is virtually eliminated, while, surprisingly, *foxd3* expression is reduced in hindbrain neural crest, but not in more anterior neural crest adjacent to the midbrain or at more posterior somite levels (Fig. 4B,D,F). Furthermore, several other genes expressed prior to this stage in the premigratory neural crest including *snail2* (*sna2*) and *sox9b* are expressed in the correct locations in *low* mutants (data not shown). By mid-migratory stages (14-18 hpf), there are dramatic reductions in *sox9b* (Fig. 4G,H), but *sna2* remains relatively unaffected, particularly when compared by two-color in situ hybridization with defects in *ctn* expression (Fig. 4I-L). These results suggest that there are distinct requirements for *tfap2a* in specification of subpopulations within the crest.

Consistent with an early role in neural crest cell specification, markers of pigment precursors are disrupted in

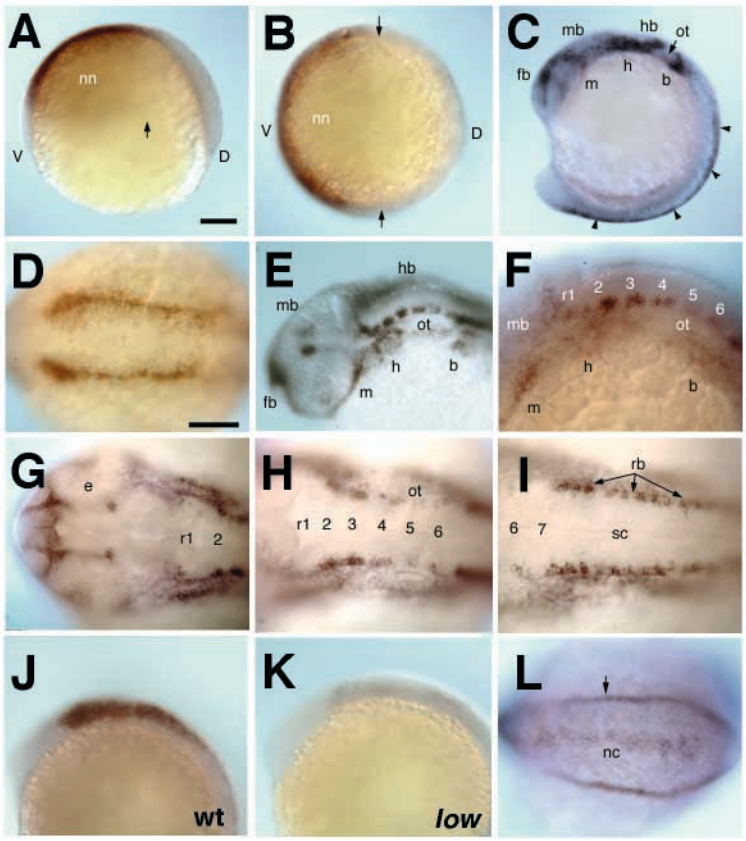

Fig. 3. *tfap2a* expression in early zebrafish embryos. Whole-mount in situ hybridization was performed with an antisense probe to *tfap2a*. (A) Lateral and (B) animal pole views of expression in the non-neural ectoderm (nn) of an 8 hpf gastrula-stage embryo. Arrows indicate boundary with neural ectoderm. (C) Lateral and (D) dorsal views, anterior towards the left, of expression in the cranial neural crest at 12 hpf (D) and at nine somites (C). Arrowheads indicate premigratory spinal neural crest. (E) Lateral view, 24 hpf; higher magnification is shown in F of segmental expression in the hindbrain and pharyngeal arches. (G-I) Dorsal views of expression in successively more posterior regions of the CNS. (G) Expression in the telencephalon and mesencephalon. (H) Segmental clusters of neurons in each rhombomere. (I) Expression in Rohon-Beard cells in the dorsal spinal cord. (J,K) Lateral views of *tfap2a* expression in premigratory neural crest in wild type (J) and a *low* mutant (K). (L) *tfap2a* expression in midline neural crest and in lateral mesoderm in the tailbud at nine somites (arrow). b, branchial; fb, forebrain; hb, hindbrain; h, hyoid; m, mandibular; mb, midbrain; nc, neural crest; nn, non-neural ectoderm; ot, otic vesicle; r1-7, rhombomeres; rb, Rohon-Beard cell; sc, spinal cord. Scale bars: 100 μm.

low mutants. In 26 hpf wild-type embryos, both *dopachrome tautomerase* (*dct*) and *kit* are expressed in melanocyte precursors just anterior and posterior to the otic vesicle, *dct* is also strongly expressed in the pigmented epithelium of the eye (Fig. 5A,C). In *low* mutants, expression of *dct* is reduced to a small cluster of post-otic crest cells at this stage, but is expressed normally in the eye (Fig. 5B), and *kit* expression is severely reduced (Fig. 5D). This is consistent with the established function of Tfap2a in regulating *kit* in other vertebrates (Huang et al., 1998). Likewise, *gch* which is expressed in both melanophore and xanthophore precursors (Fig. 5E) marks many fewer cells in *low* mutants at 24 hpf (Fig. 5F) particularly in the vicinity of the otic vesicle. We found reductions in expression of several other pigment precursor markers at this stage including *mitfa*, *endrb*, *xdh* and *fms*, and reductions in differentiated xanthophores and iridophores at 72 hpf (Lister, 2002) (data not shown), demonstrating that a proportion of all pigment cell lineages requires *tfap2a* function.

Neuronal and glial defects in *low*

Neural crest cells in the trunk form in part through lateral

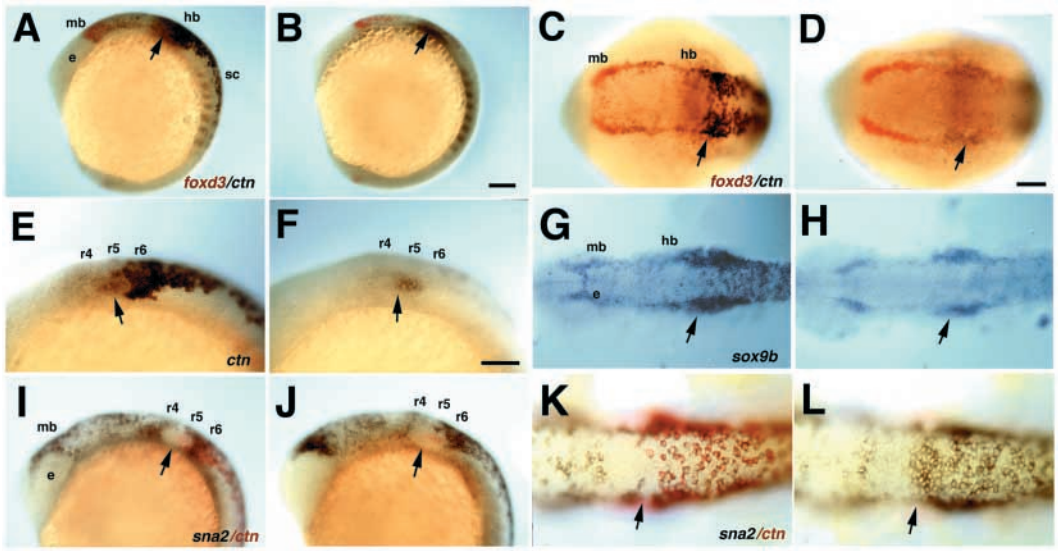

Fig. 4. Early neural crest defects in *low*^{ts213} mutants. Two-color, whole-mount in situ hybridization was performed at the six-somite (A-F) or 12-somite (G-L) stages, with antisense RNA probes to (A-D) *foxd3* and *ctn*, (E,F) *ctn* alone, (G,H) *sox9b*, and (I-L) *sna2* and *ctn* in wild-type (A,C,E,G,I,K) and *low*^{ts213} mutant (B,D,F,H,J,L) embryos. Lateral (A,B,F,I,J) and dorsal (C,D,G,H,K,L) views, anterior towards the left. Arrows indicate the otic vesicle. e, eye; mb, midbrain; hb, hindbrain; r3-6, rhombomeres 3-6; sc, spinal cord. Scale bars: 100 μm.

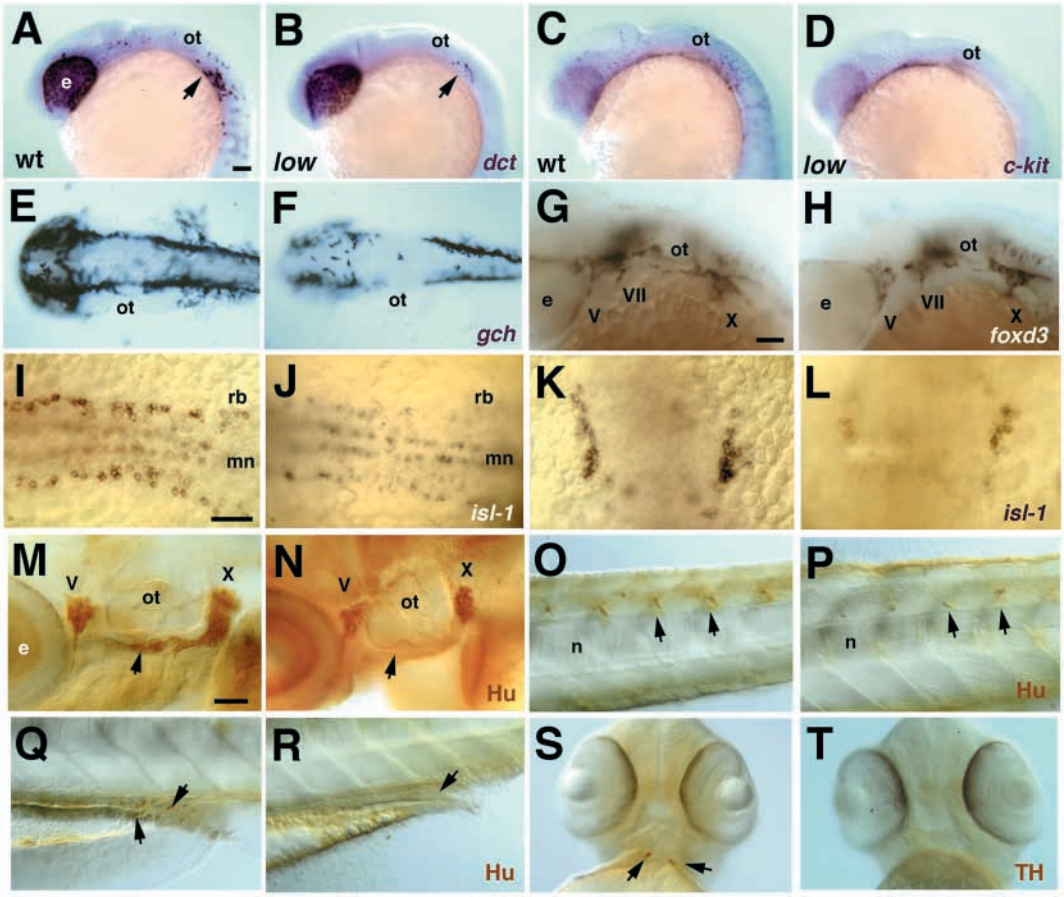

Fig. 5. Defects in pigment precursors, neuronal and glial derivatives of the neural crest. (A-H) Whole-mount in situ hybridization with riboprobes to *dct* (A,B) and *kit* (C,D) at 22 hpf (lateral views), as well as *gch* (E,F) at 25 hpf (dorsal views) and *foxd3* (G,H) at 28 hpf (lateral views) in wild-type (A,E,C,G) and *low*^{ts213} mutants (B,D,F,H). (I-L) In situ hybridization for *isl1* in wild type (I,K) and mutants (J,L) at the six-somite stage (dorsal views). (M-R) Immunostaining with anti-Hu antibody at 72 hpf (lateral views) of wild type (M,O,Q) and mutants (N,P,R) showing cranial (M,N) and spinal (O,P) ganglia (arrows), and enteric neurons (Q,R, arrows). (S,T) Immunostaining with anti-TH antibody of carotid bodies (arrows) at 60 hpf (ventral views) in wild type (S) and mutant (T). e, eye; mn, motoneurons; n, notochord; ot, otic vesicle; rb, Rohon-Beards, V, trigeminal ganglia, X, vagal ganglia. Scale bars: 100 μm.

inhibition of neurogenesis by neuroblasts that form dorsal sensory neurons (the RB cells) in the spinal cord (Cornell and Eisen, 2000; Cornell and Eisen, 2002). RB cells as well as crest cells express *tfap2a*. (Fig. 3I). RB cells form in *low* mutants, though their numbers are slightly reduced (Fig. 5I,J). In 12 hpf wild-type embryos, the transcription factor Islet1 (Isl1) marks 12-14 neural precursors in each of the trigeminal placodes (Fig. 5K), which are derived from epidermal placodes. The number is reduced to five or six cells in *low* mutants (Fig. 5L). By 36 hpf the *low* mutant trigeminal ganglion is well-formed but contains only 60-70% of the normal number of neurons (Fig. 5M,N). Other cranial ganglia, including both neural crest-derived neurons of the facial (VII), glossopharyngeal (IX) and vagal (X) nerves, as well as placodally derived epibranchial ganglia are also reduced in size and neuron number. Somewhat surprisingly, neural crest-derived glial cells in these ganglia, as assayed by expression of *foxd3* at 28 hpf are only mildly reduced in number, by ~10% (Fig. 5G,H). By 72 hpf, mutants lack enteric neurons derived from neural crest (Fig. 5Q,R), as well as sympathetic neurons (data not shown), while dorsal root ganglia are less affected (Fig. 5O,P). Tyrosine hydroxylase (TH)-positive neurons of the carotid bodies, which form just ventral to the hyoid arch, are also reduced in *low* (Fig. 5S,T), as are other TH-positive neurons in the CNS (data not shown). Thus, neuronal defects in *low* mutants include a variety of sensory neurons derived from both neural crest, and epidermal placodes, but spare many sensory neurons and glia of cranial and spinal ganglia.

Neural crest migration and survival in *low*

The changes in gene expression in the neural crest of *low* could reflect a downregulation of target gene expression or, alternatively, a failure of neural crest cells to migrate, proliferate or survive. To distinguish between these possibilities, we followed cranial neural crest morphogenesis in living *low* mutant embryos (Fig. 6A-D). Morphological inspection with Nomarski optics at 24 hpf revealed the presence of reduced arch primordia within which cells appear disorganized and not arranged in linear rows as in wild type (data not shown). To examine the segmental origins of these disorganized arches, we followed labeled neural crest cells in *low* mutants using the fate map for premigratory neural crest

generated for 12 hpf embryos (Schilling and Kimmel, 1994). The photoactivatable dye DMNB-caged fluorescein was injected into the progeny of *low* heterozygotes at the one-cell stage and the dye was UV-activated in a local region of the cranial neuroepithelium when embryos reached the eight- to ten-somite stage. This technique typically labeled both neural tube and neural crest cells, marking the segmental origins of the crest cells. In both wild-type and *low* mutant embryos, fluorescent cells were found to migrate to the appropriate pharyngeal arch. For example, photoactivation in the region immediately posterior to the eye labels stream I and later the mandibular arch (Fig. 6A,B), while labeling just anterior or posterior to the otic vesicle labels stream II and the hyoid or stream III and the branchial arches, respectively (Fig. 6A-D). These results suggest that *low* mutant neural crest cells migrate and roughly populate the appropriate segments along the anteroposterior axis.

To determine if *low* is required for neural crest cell survival, we analyzed cell death patterns in wild-type and *low* homozygous embryos using TUNEL analysis (Fig. 6E-G). Strikingly, although fewer than 10 TUNEL-positive cells were typically observed in wild-type embryos, by the six-somite stage, 30-90 TUNEL-positive cells/embryo were observed in the dorsal ectoderm at all anteroposterior levels in 25% of embryos derived from an intercross between *low* heterozygotes (Fig. 6E,F). At slightly earlier stages, labeling was restricted to midbrain/hindbrain levels, correlated with the timing of neural crest emigration (data not shown). Furthermore, by the 12-somite stage, the number of dying cells in the cranial region had decreased, and labeling spread to spinal levels (Fig. 6I). TUNEL labeling subsequently became less pronounced by late segmentation stages. Some TUNEL-positive cells at the six-somite stage were identified as neural crest cells by colocalization with the few remaining *ctn*-positive cells in *low*, and this further confirmed that the death occurs specifically in *low* mutants (Fig. 6G,H). Thus at least some neural crest cells require *low* (*tfap2a*) function for their survival, and this requirement appears to be limited to a short early period of neural crest development.

Segment-specific requirements for *low* in the cranial neural crest

The mandibular arch is much less affected in *low* mutants than other pharyngeal arches, and in some cases the first and second arch cartilages appear to fuse, reminiscent of a homeotic transformation of the second arch into a first arch identity (Fig. 1) (Hunter and Prince, 2002). In wild-type embryos at 32 hpf, *dlx2* is strongly expressed in five out of the eventual seven pharyngeal arches as well as in the forebrain (Fig. 7A,C). In *low* mutants, only expression in the mandibular and weak expression in some branchial arches can be detected, yet the mandibular expression domain is approximately the normal size and shape (Fig. 7B,D). Mandibular neural crest is Hox negative, in contrast to crest migrating into the hyoid arch, which expresses Hox group 2 genes. To determine if the pharyngeal arch defects in *low* are due to disruption of Hox gene expression we examined the expression of *hoxa2* and *hoxb2* at 28 hpf. Both are

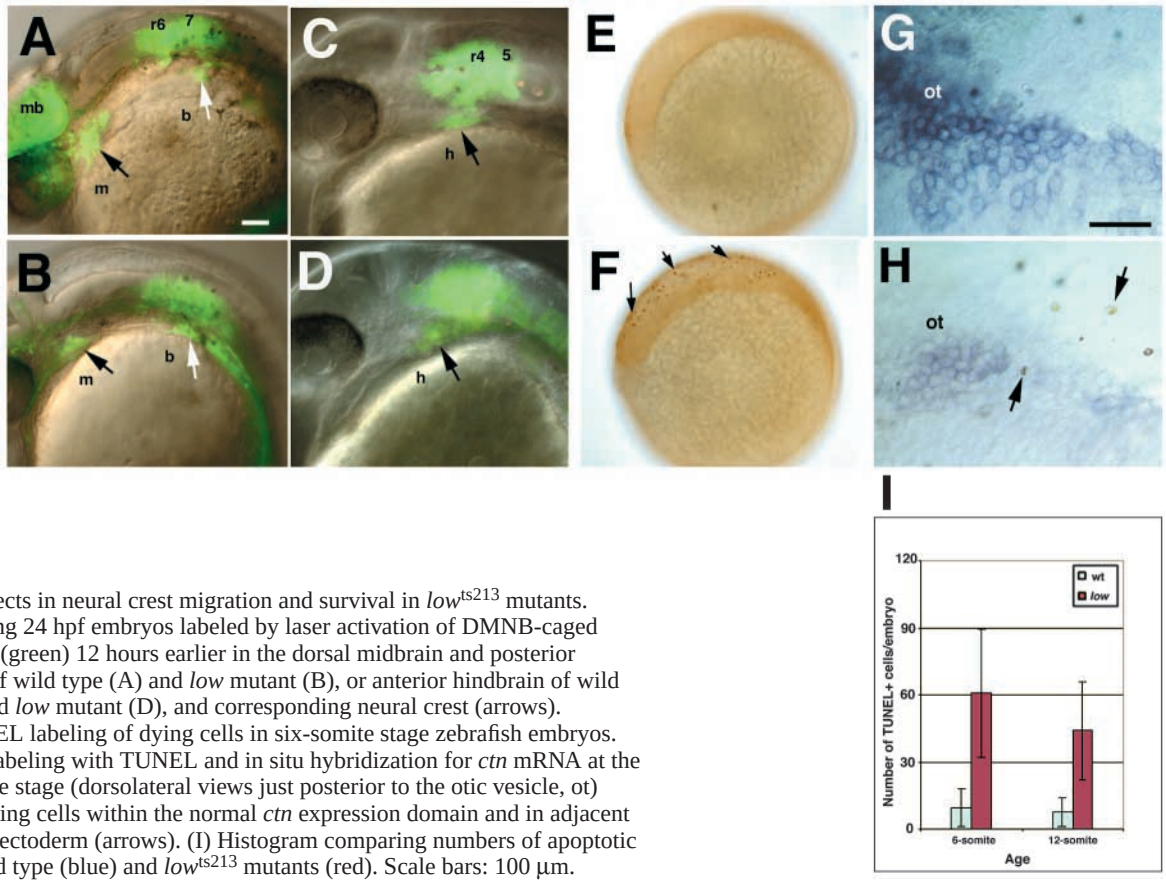

Fig. 6. Defects in neural crest migration and survival in *low*^{ts213} mutants. (A-D) Living 24 hpf embryos labeled by laser activation of DMNB-caged fluorescein (green) 12 hours earlier in the dorsal midbrain and posterior hindbrain of wild type (A) and *low* mutant (B), or anterior hindbrain of wild type (C) and *low* mutant (D), and corresponding neural crest (arrows). (E,F) TUNEL labeling of dying cells in six-somite stage zebrafish embryos. (G,H) Co-labeling with TUNEL and in situ hybridization for *ctn* mRNA at the eight-somite stage (dorsolateral views just posterior to the otic vesicle, ot) showing dying cells within the normal *ctn* expression domain and in adjacent non-neural ectoderm (arrows). (I) Histogram comparing numbers of apoptotic cells in wild type (blue) and *low*^{ts213} mutants (red). Scale bars: 100 μm.

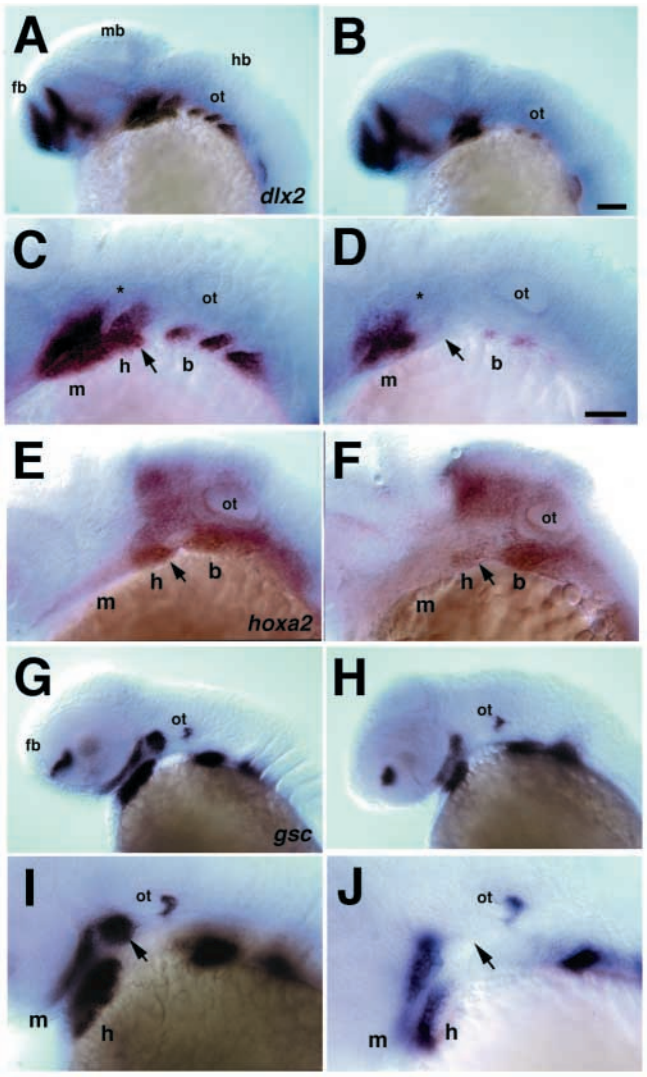

Fig. 7. Defects in pharyngeal arch development in *low*^{ts213} mutants. Whole-mount in situ hybridization with riboprobes to *dlx2* (A-D) and *hoxa2* (E,F) at 28 hpf, as well as *gsc* (G-J) at 40 hpf. Wild type (A,C,E,G,I); mutant (B,D,F,H,J). Lateral views, anterior towards the left. Arrows in C-F indicate the hyoid arch. Arrows in I and J indicate the dorsal expression domain of *gsc*, which is absent in *low*^{ts213}. b, branchial arches, fb, forebrain, h, hyoid arch, hb, hindbrain, m, mandibular arch, mb, midbrain, ot, otic vesicle. Scale bars: 100 μm.

dramatically reduced in the hyoid arch in *low* mutants, but not in the hindbrain (Fig. 7E,F). This is similar to results from analyses of the enhancer elements driving mouse *Hoxa2* expression in the hyoid neural crest, which are regulated by AP2 genes (Maconochie et al., 1999). Defects in the hyoid arch are most severe dorsally with loss of the hyosymplectic and fusion of its remnant with the mandibular skeleton. This correlates with a loss of *gsc* expression in the dorsal hyoid at 36 hpf (Fig. 7G-J) (Miller at al., 2000). A loss of Hox2 group genes in the second arch, coupled with the loss of *dlx2* and *gsc* could account for some of the segmental fusions and abnormal jaw articulations we observe in *low* mutants.

Cell autonomous requirements for *low* in neural crest formation

Tcfap2a is expressed throughout the ectoderm and required for neural tube closure in mice (Schorle et al., 1996; Zhang et al., 1996) as well as playing important roles in epidermis development in both *Xenopus* and mice (Pfisterer et al., 2002; Luo et al., 2002). Thus, neural crest defects in *low* mutants might be caused indirectly by defects in other ectodermal derivatives. To exclude this possibility, we used mosaic analysis to test the capacity of wild-type cells to rescue the mutant phenotype when surgically transplanted into the second pharyngeal arch (Fig. 8). Premigratory neural crest that forms this arch has been mapped just anterior to the otic vesicle at 12 hpf (Schilling and Kimmel, 1994). Cranial neural crest cells were transplanted from this location in a biotin-labeled donor at 12 hpf into the same region on one side of the neural crest of an unlabeled host and their fates followed until 72 hpf (n=24; Fig.8 A-C) (see Schilling et al., 1996b). The untransplanted side served as a control and allowed unambiguous identification of the host as mutant or wild type. Wild-type cells transplanted into wild-type hosts often contributed neurons to rhombomeres 4 and 5 of the hindbrain as well as a stream of neural crest within the hyoid arch (Fig. 8A-A″). Similar transplants from wild-type donors into *low* mutant hosts also resulted in large numbers of crest cells in the hyoid (Fig. 8B-B″), and in some cases this also restored cartilage and muscle differentiation in the hyoid arch (Fig. 8B‴), revealing non-autonomous requirements for low in mesodermally derived muscles that require interactions with skeletogenic crest cells (Noden, 1983; Schilling et al., 1996a). By contrast, *low* mutant cells transplanted into wild-type hosts often failed to migrate and never formed cartilage (n=12; Fig. 8C,C′). These results demonstrate that *low* acts cell autonomously in the cranial neural crest.

Discussion

lockjaw is a zebrafish *tfap2a* mutant

In this study, we show that *lockjaw* (*low*) is due to a mutation in a zebrafish AP2 gene, orthologous to mammalian *Tcfap2a*, and is required for early patterning of the neural crest. The lesion in *low* is a point mutation in *tfap2a* that introduces a stop codon in the highly conserved DNA-binding domain, and is predicted to cause a complete loss of function, based on studies in cell culture (Garcia et al., 2000). Consistent with this, injection of two antisense morpholino oligonucleotides directed against splicing sites in *tfap2a* phenocopies *low* but does not give a more severe phenotype, indicating that *low* is a complete loss of *tfap2a* function. Disruption of *Tcfap2a* function in mice causes defects in the neural crest-derived craniofacial skeleton and cranial ganglia (Schorle et al., 1996; Zhang et al., 1996). Our analysis of *low* reveals a conserved role for *tfap2a* in vertebrates in patterning the cranial neural crest and has implications for understanding human craniofacial and deafness syndromes. We propose a model in which *tfap2a* is required for (1) early patterning of subpopulations of the neural crest and (2) segment-specific patterning of the hyoid arch (Fig. 9).

tfap2a and neural crest cell survival

In the *Tcfap2a* mutant mouse, extensive cell death in the neural

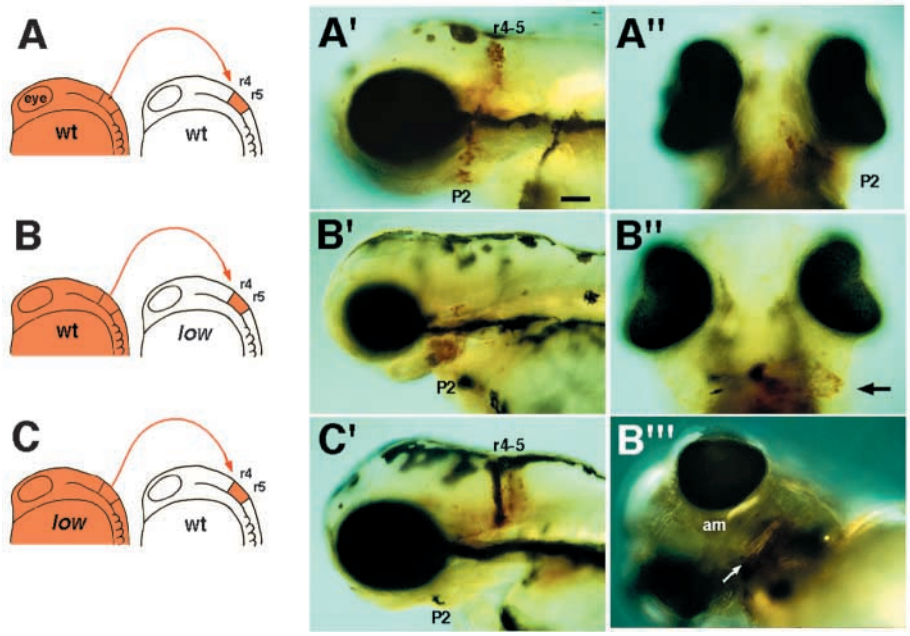

Fig. 8. Transplants suggest that *low*^{ts213} functions cell autonomously in neural crest. Prospective hyoid arch neural crest and hindbrain cells at the level of rhombomeres 4 and 5 (r4 and r5) were transplanted from donor embryos labeled with a lineage tracer (red) into unlabeled hosts at 12 hpf (A-C). Lateral views (A′-C′) and ventral views (A″-C″) of mosaic larvae at 65 hpf stained for biotinylated tracer (brown). (A-A″) Control transplants between wild-type embryos. (B-B″) Wild-type transplants into *low* mutants. Arrow indicates rescued hyoid arch outgrowth on the transplanted side. (C,C′) Transplants of *low* mutant crest cells into wild-type hosts. (B‴) Rescued muscles of the hyoid arch in *low* mutants containing transplanted wild-type neural crest. am, adductor mandibulae muscle; P2, pharyngeal arch 2 (hyoid arch). Scale bars: 100 μm.

folds and in the mesenchyme of the pharyngeal arches has been suggested to cause the craniofacial phenotype (Schorle et al., 1996). We also observe increased apoptosis in the cranial region of *low* at early segmentation stages, indicating a conserved function of *tfap2a* in cell survival and suggesting a cause for the *low* phenotype.

This function in preventing apoptosis is conserved between other vertebrate and *Drosophila* AP2 genes (Kerber et al., 2001). AP2 proteins form a complex with retinoblastoma protein to activate transcription of *Bcl2* in mammalian epithelial cells, which directly prevents apoptosis (Decary et al., 2002) and can also prevent apoptosis through inhibition of DNA binding by the cell-cycle progression factor Myc (Hilger-Eversheim et al., 2000). These established roles for AP2 proteins in promoting cell survival suggest that the *low* phenotype may be due to increased neural crest cell death following loss of *tfap2a* function. In support of this, we found that some dying cells in *low* express *ctn*, a neural crest-specific marker. Apoptosis occurs throughout the neural crest and in the dorsal epidermis, but occurs only during a brief interval of development, between 12-15 hpf, which might account for the partial loss of neural crest derivatives. These results suggest that the *low* phenotype might be explained by apoptosis.

An alternative hypothesis for the *low* phenotype is that some neural crest is not specified correctly early in development, resulting in an absence of a subset of pigment and skeletal cells. In support of this, a number of early neural crest markers are reduced or absent in premigratory cranial neural crest cells of *low*, but expression of *Sna2* (orthologous to mammalian *Snail*), is unaffected in the same cells. The expression of *Snail2* is also unaffected at stages in which we observe most apoptosis in putative neural crest, suggesting that many neural crest cells remain in *low*. Given the very early role of the *Snail* gene family in neural crest specification and migration in *Xenopus* and chick (LaBonne and Bronner-Fraser, 1998; del Barrio et al., 2002) (reviewed by Nieto, 2002), this suggests that neural crest cells are specified in *low*, but later patterning is disrupted, possibly leading to apoptosis. These early expression defects of some genes in the neural crest of *low* correlate with later differentiation of a subset of neural crest derivatives. Thus, in this model we would argue that the loss of certain subpopulations of neural crest in *low* is a direct result of early patterning defects. This model does not preclude death of these cells by apoptosis at later stages, although we do not have direct evidence that the gene expression defects and patterns of apoptosis are related. Rather apoptosis, when it occurs, appears widespread in *low* and not confined to any particular regions of the head, as might be expected if death accounted for the regional defects in neural crest in the arches.

low reveals a cell autonomous role of *tfap2a* in specifying neural crest subpopulations

Neural crest cells form many different cell types after migration from the neural tube, and interactions between these migrating cells and their environment are known to regulate crest cell fates (LeDouarin, 1982; Noden, 1983; Graham and Smith, 2001). In order to show whether the pigment, neuronal and skeletal defects in *low* are due to a disruption in signals from their environment or a result of a cell intrinsic defect in the neural crest, we performed transplants of neural crest between wild type and *low*. These transplants show that *tfap2a* is required in a cell-autonomous manner for at least a subset of neural crest to migrate and contribute to the pharyngeal arches. In some cases, wild-type crest cells alone rescued surrounding pharyngeal muscles in low, revealing interactions between skeletogenic crest and surrounding mesodermally derived muscles (Noden, 1983; Schilling et al., 1996a). Transplanted neural crest cells taken from *low* mutants showed reduced migration into wild-type arches, yet many of these cells appeared to migrate normally. This was supported by photoactivation of fluorescein in premigratory neural crest cells in *low*, many of which then migrated normally into the pharyngeal arches. These results do not resolve which particular subset of neural crest is affected in *low*, an issue that

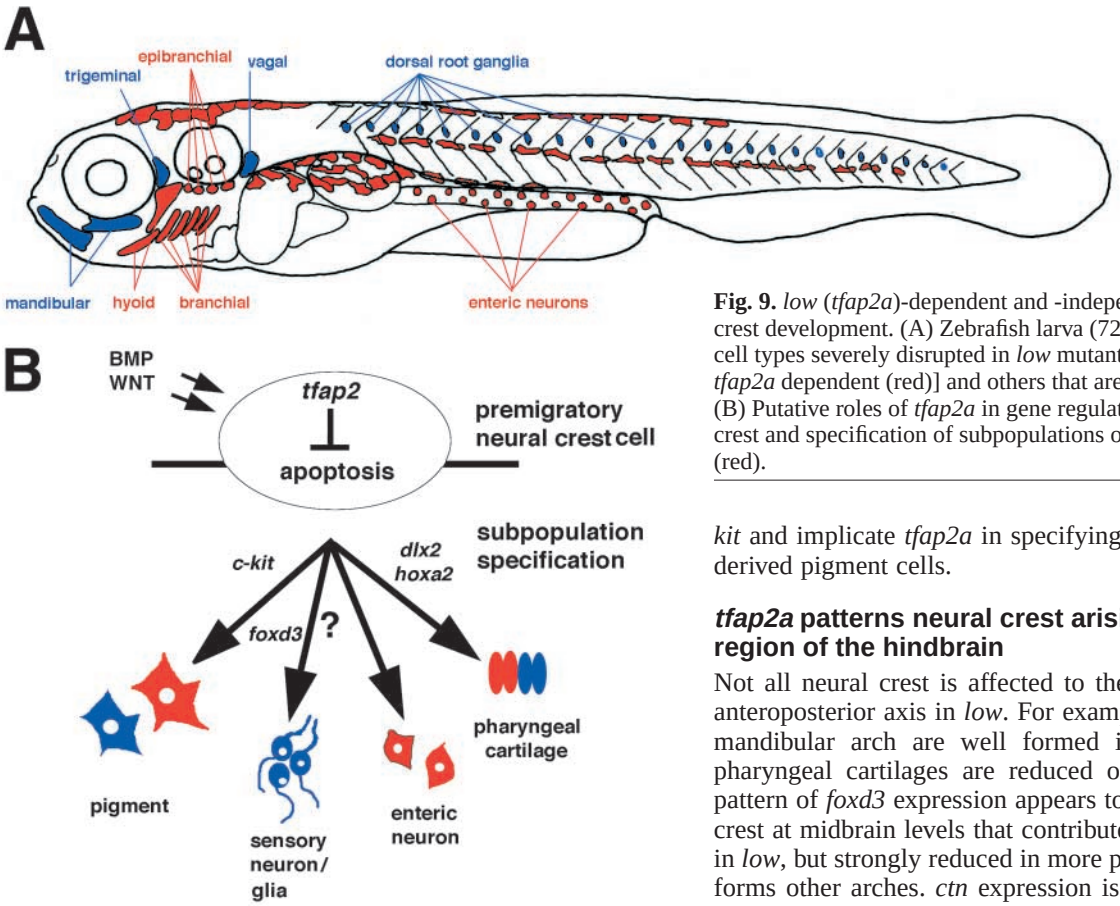

Fig. 9. *low* (*tfap2a*)-dependent and -independent aspects of neural crest development. (A) Zebrafish larva (72 hpf) and the locations of cell types severely disrupted in *low* mutants [and therefore largely *tfap2a* dependent (red)] and others that are less effected (blue). (B) Putative roles of *tfap2a* in gene regulation in the premigratory crest and specification of subpopulations of neural crest derivatives (red).

will require lineage analyses of individual crest cells, but they do suggest that *tfap2a* function is only required in some of these cells.

In zebrafish, the most lateral premigratory neural crest cells that migrate early form neurons, in contrast to more medial cells (which will form pigment cells and cartilage) (Schilling and Kimmel, 1994; Raible and Eisen, 1994). One explanation for the differential affects on neural crest-derived cells in *low*, is that *tfap2a* is only required during a short period of crest development, perhaps only in early or late migrating cells. Supporting this hypothesis, neural crest-derived neurons and glia of the dorsal root and cranial ganglia are only mildly disrupted in *low*, in contrast to pigment cells and craniofacial cartilages which are severely reduced.

Even among pigment or cartilage derived from neural crest, only subpopulations appear to require *low* function, suggesting a more restricted role of *tfap2a*. For example, melanocytes are heavily reduced in *low*, in contrast to xanthophores or iridophores, which are less affected. Consistent with this, genes expressed exclusively in melanoblasts (*kit*, *dct*) are more severely affected in *low* than others reported to be expressed in both melanoblasts and xanthophores (*gch*) (Parichy et al., 1999; Kelsh et al., 2000; Pelletier et al., 2001). In mammals, the proto-oncogene *Kit* is directly regulated by AP2 genes, and in zebrafish a homolog of this gene has been shown to have a crucial role in melanoblast development (Baldi et al., 2001; Parichy et al., 1999). Our data point to a conserved function of *tfap2a*. in melanocyte development through the regulation of *kit* and implicate *tfap2a* in specifying subsets of neural crest-derived pigment cells.

tfap2a patterns neural crest arising from a restricted region of the hindbrain

Not all neural crest is affected to the same extent along the anteroposterior axis in *low*. For example, the cartilages of the mandibular arch are well formed in mutants while other pharyngeal cartilages are reduced or absent. Likewise, the pattern of *foxd3* expression appears to be unaffected in neural crest at midbrain levels that contribute to the mandibular arch in *low*, but strongly reduced in more posterior neural crest that forms other arches. *ctn* expression is only mildly reduced in the trunk in mutants but absent from cranial neural crest migrating adjacent to the otic vesicle. Both neural crest of the ectomesenchymal lineage (which forms cartilage) and pigment precursors are affected at this position, as shown by a striking loss of all *gch*+ pigment precursors at the level of the otic vesicle, as well as loss of *sox9b*- and *dlx2*-expressing presumptive skeletogenic cells.

The neural crest that arises immediately adjacent to the otic vesicle, in rhombomeres 4 and 5, migrates anterior to the otic vesicle into the hyoid arch, whereas neural crest from more posterior rhombomeres migrates posterior to the otic vesicle into the branchial arches (Schilling and Kimmel, 1994). The regional defects in neural crest expression during their migration into the arches of *low*, suggest that *tfap2a* is required for patterning of a population of neural crest which arise from a restricted region of the hindbrain. This correlates with segment-specific defects in pharyngeal cartilages; while the hyoid arch is severely disrupted in all cases, the mandibular arch is only slightly reduced. More posterior branchial arches are consistently present but reduced in *low*.

One significant feature of neural crest migrating into the hyoid and more posterior arches, is that they express Hox group 2 genes, in contrast to neural crest that forms the mandibular arch (Hunt et al., 1991; Prince and Lumsden, 1994). *Hoxa2*, in particular, has been shown to be required for the segmental identity of the hyoid arch, which undergoes a partial transformation to a mandibular morphology in *Hoxa2* mutant mice (Rijli et al., 1993; Gendron-Maguire et al., 1993). In *low*, both *hoxa2* and *hoxb2* expression are severely reduced in the hyoid and branchial arches, suggesting that *tfap2a*

regulation of Hox genes may be an essential requirement in correct patterning of the cranial neural crest. Although we have not found clear evidence for segmental transformations, as observed in *Hoxa2* mutant mice, some of the arch fusions and abnormal jaw articulations observed in *low* may occur as a consequence of loss of expression of Hox2 group genes. Furthermore, we have not detected defects in expression of *hoxa2* or *hoxb2* in the hindbrain or in patterning of rhombomeres in *low*, consistent with an independent regulation in the CNS and in neural crest (Prince and Lumsden, 1994; Maconochie et al., 1999; Tumpel et al., 2002). Analysis of enhancer elements in mouse *Hoxa2* has shown a requirement for AP2 genes in regulating expression of *Hoxa2* in hyoid and branchial arch neural crest (Maconochie et al., 1999). Our results indicate that regulation of Hox group 2 gene expression in neural crest is a conserved function of *tfap2a* in vertebrates, and we propose that the defects in the craniofacial skeleton of *low* are a direct result of loss of Hox gene function.

However, this loss of Hox group 2 expression is not complete, as shown by reduced ventral expression of *hoxa2* in the hyoid and branchial arches, but appears to be specific to the dorsal arch. This dorsal specific defect is even more apparent in the loss of *gsc* expression specifically in the dorsal hyoid arch. This loss of dorsal hyoid arch expression may account for the cartilage phenotype in *low*, in which the dorsal element of the hyoid, the hyposymplectic is absent. Interestingly, this segmental restriction of *tfap2a* function in patterning the hyoid, may also be conserved in vertebrates, as it has been reported that in a mouse *Tcfap2a* null background, ventrally restricted expression of a *Hoxa2* enhancer construct is still present (Maconochie et al., 1999). It is interesting to speculate as to how dorsoventral specificity arose in the pharyngeal arches, as the putative vertebrate ancestor is proposed to have had unjointed arches that show no regional differences along the DV axis, as evidenced for an agnathan, lamprey (de Beer, 1937). Independent regulation of patterning genes in the dorsal and ventral arch may have allowed the innovation of novel vertebrate structures, such as jaws.

tfap2a is an early, essential gene in neural crest development

Neural crest originated after the divergence of cephalochordates and vertebrates, commensurate with an increase in genome complexity and gene number (Shimeld and Holland, 2000). AP2 expression in neural crest is basal to the vertebrate lineage, implying a conserved function of these genes in neural crest development that arose at the origin of vertebrates (Meulemans and Bronner-Fraser, 2002). Disruption of *Tcfap2a* gene function in mice revealed an essential role in neural crest survival, in addition to neural tube closure and middle ear development (Schorle et al., 1996; Zhang et al., 1996). We show that a zebrafish mutant in *tfap2a* displays similar defects in neural crest-derived tissues as those seen in the mouse *Tcfap2a* mutant. However, we have not detected similar defects in other ectodermal derivatives such as the neural tube, possibly reflecting differences in its development between fish and mouse.

In addition, we document a surprisingly early disruption of neural crest in *low* mutants, prior to migration, unlike that described in the mouse. Apoptosis in the neural crest of the pharyngeal arches was proposed as the cause of the mutant mouse phenotype, but no defects in neural crest migration or expression of early markers was described. We show that loss of *tfap2a* function in zebrafish disrupts early patterning of several populations of neural crest cells that form pigment, neurons and cartilage. Differences between the mouse and zebrafish mutants may be due to compensation by other AP2 genes in the mouse, such as *Tcfap2b*, which are expressed in the neural crest and may compensate for loss of *Tcfap2a* function. However, double mutant *Tcfap2a*/*Tcfap2b* mice still do not show early neural crest defects (T. Williams, personal communication). Alternatively, heterochronic differences in the timing of neural crest development of mouse compared with zebrafish might account for the observation that mouse *Tcfap2a* has a later function in pharyngeal arch neural crest development. We believe this unlikely, however, as such similar sets of neural crest derivatives are affected in mouse and zebrafish, all with a common origin in the hindbrain, implying an early requirement for *tfap2a* in their development. More detailed analyses of genes expressed in the neural crest in *Tcfap2a* mutant mice, should resolve these issues.

An important consequence of disruption of *tfap2a* function, is the loss of Hox group 2 gene expression in the hyoid and branchial arches. This requirement for *tfap2a* function in regulating Hox group 2 expression is conserved between mouse and zebrafish, and both mutants show disruption of the cartilages that in mammals give rise to the bones of the middle ear. Mice that are mutant for *Tcfap2a* display a range of phenotypes in which the middle ear bones are reduced or malformed (K. B. Avraham and K. P. Steel, personal communication). Human *TFAP2A* maps to chromosome 6p24.2 and a number of deafness syndromes have been mapped near to this location (Law et al., 1998). Furthermore, an individual has been described in whom *TFAP2A* is deleted, who has a reduced jaw, microphthalmia, proximally positioned thumbs and abnormal ear morphology (Davies et al., 1999). This suggests that *Tfap2a* has a highly conserved role in vertebrate development with many implications for human craniofacial and deafness syndromes.

We thank P. Ingham for support in the early stages of this work and P. Boardman for technical assistance. We also thank T. Williams and members of our laboratory for stimulating discussions and critical reading of the manuscript. R.G. and G.J.-R. thank Silke Rudolph-Geiger for technical assistance. We are grateful to J. Holzschuh, W. Driever, T. Williams and R. Cornell for communication of unpublished results. C. Amemiya provided arrayed PAC genomic libraries. We would like to thank the following people for probes: S. Johnson, J. Lister, V. Prince and D. Raible. This work was supported by the NIH (NS-41353, DE-13828), March of Dimes (1-FY01-198) and Pew Scholars Foundation (2615SC) to T.S., and by the German Human Genome Project (DHGP Grant 01 KW 9919).

REFERENCES

Akimenko, M. A., Ekker, M., Wegner, J., Lin, W. and Westerfield, M. (1994). Combinatorial expression of three zebrafish genes related to *distal-less*: part of a homeobox gene code for the head. *J. Neurosci.* **14**, 3475-3486.

Amemiya, C. T., Zhong, T. P., Silverman, G. A., Fishman, M. C. and Zon, L. I. (1999). Zebrafish YAC, BAC and PAC genomic libraries. *Methods Cell Biol.* **60**, 235-258.

Amores, A., Force, A., Yan, Y.-L., Joly, L., Amemiya, C., Fritz, A., Ho, R. K., Langeland, J., Prince, V., Wang, Y.-L. et al. (1998). Zebrafish hox clusters and vertebrate genome evolution. *Science* **282**, 1711-1714.

Aybar, M. J. and Mayor, R. (2002). Early induction of neural crest cells: lessons learned from frog, fish and chick. *Curr. Opin. Genet. Dev.* **12**, 452-458.

Baldi, A., Santini, D., Battista, T., Dragonetti, E., Ferranti, G., Petitti, T., Groeger, A. M., Angelini, A., Rossiello, R., Baldi, F. et al. (2001). Expression of AP-2 transcription factor and of its downstream target genes c-kit, E-cadherin and p21 in human cutaneous melanoma. *J. Cell Biochem.* **83**, 364-372.

Brewer, S., Jiang, X., Donaldson, S., Williams, T. and Sucov, H. M. (2002). Requirement for AP-2alpha in cardiac outflow tract morphogenesis. *Mech. Dev.* **110**, 139-149.

Chazaud, C., OuladAbdelghani, M., Bouillet, P., Decimo, D., Chambon, P. and Dolle, P. (1996). AP-2.2, a novel gene related to AP-2, is expressed in the forebrain, limbs and face during mouse embryogenesis. *Mech. Dev.* **54**, 83-94.

Christiansen, J. H., Coles, E. G. and Wilkinson, D. G. (2000). Molecular control of neural crest formation, migration and differentiation. *Curr. Opin. Cell Biol.* **12**, 719-724.

Cornell, R. A. and Eisen, J. S. (2000). Delta signaling mediates segregation of neural crest and spinal sensory neurons from zebrafish lateral neural plate. *Development* **127**, 2873-2882.

Cornell, R. A. and Eisen, J. S. (2002). Delta/Notch signaling promotes formation of zebrafish neural crest by repressing Neurogenin 1 function. *Development* **129**, 2639-2648.

David, N. B., Saint-Etienne, L., Tsang, M., Schilling, T. F. and Rosa, F. M. (2002). Requirement for endoderm and FGF3 in ventral head skeleton formation. *Development* **129**, 4457-4468.

Davies, A. F., Mizra, G., Flinter, F. and Ragoussis, J. (1999). An interstitial deletion of 6p24-p25 proximal to the *FKHL7* locus and including *AP-2α* that affects anterior eye chamber development. *J. Med. Genet*. **36**, 708-710.

de Beer, G. (1937). *The Development of the Vertebrate Skull*. Oxford: Oxford University Press.

Decary, S., Decesse, J. T., Ogryzko, V., Reed, J. C., Naguibneva, I., Harel-Bellan, A. and Cremisi, C. E. (2002). The retinoblastoma protein binds the promoter of the survival gene bcl-2 and regulates its transcription in epithelial cells through transcription factor AP-2. *Mol. Cell. Biol.* **22**, 7877-7888.

del Barrio, M. G. and Nieto, M. A. (2002). Overexpression of Snail family members highlights their ability to promote chick neural crest formation. *Development* **129**, 1583-1593.

Dorsky, R. I., Moon, R. T. and Raible, D. W. (1998). Control of neural crest cell fate by the Wnt signaling pathway. *Nature* **396**, 370-373.

Dottori, M., Gross, M. K., Labosky, P. and Goulding, M. (2001). The winged helix factor FoxD3 suppresses interneuron differentiation and promotes neural crest cell fate. *Development* **128**, 4127-4138.

Endo, Y., Osami, N. and Wakamatsu, Y. (2002). Bimodal function of Notch-mediated signaling are involved in neural crest formation during avian ectodermal development. *Development* **129**, 863-873.

Epstein, D. J., Vekemans, M. and Gros, P. (1991). *Splotch* (*Sp2H*) a mutation affecting the development of the mouse neural tube shows a deletion within the paired homeodomain of Pax3. *Cell* **67**, 767-774.

Epstein, J. A. (2001). Developing models of DiGeorge syndrome. *Trends Genet.* **17**, 13-17.

Fishman, M. C., Stainier, D. Y., Breitbart, R. E. and Westerfield, M. (1997). Zebrafish: genetic and embryological methods in a transparent vertebrate embryo. *Methods Cell Biol.* **52**, 67-82.

Furthauer, M., Thisse, C. and Thisse, B. (1997). A role for FGF-8 in the dorsoventral patterning of the zebrafish gastrula. *Development* **124**, 4253-4264.

Garcia, M. A., Campillos, M., Ogueta, S., Valdivieso, F. and Vazquez, J. (2000). Identification of amino acid residues of transcription factor AP-2 involved in DNA binding. *J. Mol. Biol.* **301**, 807-816.

Garcia-Castro, M. I., Marcelle, C. and Bronner-Fraser, M. (2002). Ectodermal Wnt function as a neural crest inducer. *Science* **297**, 848-851.

Geisler, R. (2002). Mapping and cloning. In *Zebrafish: A Practical Approach* (ed. C. Nusslein-Volhard and R. Dahm), pp. 175-212. Oxford: Oxford University Press.

Graham, A. and Smith, A. (2001). Patterning the pharyngeal arches. *BioEssays* **23**, 54-61.

Gendron-Maguire, M., Mallo, M., Zhang, M. and Gridley, T. (1993). Hoxa-2 mutant mice exhibit homeotic transformation of skeletal elements derived from cranial neural crest. *Cell* **75**, 1317-1331.

Guo, S., Brush, J., Teraoka, H., Goddard, A., Wilson, S. W., Mullins, M. C. and Rosenthal, A. (1999). Development of noradrenergic neurons in the zebrafish hindbrain requires BMP, FGF8, and the homeodomain protein soulless/Phox2a. *Neuron* **24**, 555-566.

Hilger-Eversheim, K., Moser, M., Schorle, H. and Buettner, R. (2000). Regulatory roles of AP-2 transcription factors in vertebrate development, apoptosis and cell-cycle control. *Gene* **260**, 1-12.

Huang, S., Jean, D., Luca, M., Tainsky, M. A. and Bar-Eli, M. (1998). Loss of AP-2 results in downregulation of c-KIT and enhancement of melanoma tumorigenicity and metastasis. *EMBO J.* **17**, 4358-4369.

Hunt, P., Wilkinson, D. and Krumlauf, R. (1991). Patterning the vertebrate head: murine Hox 2 genes mark distinct subpopulations of premigratory and migrating cranial neural crest. *Development* **112**, 43-50.

Hunter, M. P. and Prince, V. E. (2002). Zebrafish hox paralogue group 2 genes function redundantly as selector genes to pattern the second pharyngeal arch. *Dev. Biol.* **247**, 367-389.

Inoue, A., Takahashi, M., Hatta, K., Hotta, Y. and Okamoto, H. (1994). Developmental regulation of *islet-1* mRNA expression during neuronal differentiation in embryonic zebrafish. *Dev. Dyn.* **199**, 1-11.

Isogai, S., Horiguchi, M. and Weinstein, B. M. (2001). The vascular anatomy of the developing zebrafish: an atlas of embryonic and early larval development. *Dev. Biol.* **230**, 278-301.

Kelsh, R. N., Schmid, B. and Eisen, J. S. (2000). Genetic analysis of melanophore development in zebrafish embryos. *Dev. Biol.* **225**, 277-293.

Kelsh, R. N. and Raible, D. W. (2002). Specification of zebrafish neural crest. *Results Prob. Cell Diff.* **40**, 216-236.

Kerber, B., Monge, I., Mueller, M., Mitchell, P. J. and Cohen, S. M. (2001). The AP-2 transcription factor is required for joint formation and cell survival in Drosophila leg development. *Development* **128**, 1231-1238.

Kimmel, C. B., Ballard, W. W., Kimmel, S. R., Ullmann, B. and Schilling, T. F. (1995). Stages of embryonic development of the zebrafish. *Dev. Dyn.* **203**, 253-310.

Kimmel, C. B., Miller, C. T., Kruze, G., Ullmann, B., BreMiller, R. A., Larison, K. D. and Snyder, H. C. (1998). The shaping of pharyngeal cartilages during early development of the zebrafish. *Dev. Biol.* **203**, 245-263.

Kontges, G. and Lumsden, A. (1996). Rhombencephalic neural crest segmentation is preserved throughout craniofacial ontogeny. *Development* **122**, 3229-3242.

Kos, R., Reedy, M. V., Johnson, R. L. and Erickson, C. A. (2001). The winged helix transcription factor FoxD3 is important for establishing the neural crest lineage and repressing melanogenesis in avian embryos. *Development* **128**, 1467-1479.

LaBonne, C. and Bronner-Fraser, M. (1998). Neural crest induction in Xenopus: evidence for a two-signal model. *Development* **125**, 2403-2414.

Law, C. J., Fisher, A. M. and Temple, I. K. (1998). Distal 6p deletion syndrome: a report of a case with anterior chamber eye anomaly and review of published reports. *J. Med. Genet.* **35**, 685-689.

LeDouarin, N. M. (1982). *The Neural Crest*. Cambridge, UK: Cambridge Univ. Press.

Li, M., Zhao, C., Wang, Y., Zhao, Z. and Meng, A. (2002). Zebrafish *sox9b* is an early neural crest marker. *Dev. Genes Evol.* **212**, 203-206.

Lister, J. A., Robertson, C. P., Lepage, T., Johnson, S. L. and Raible, D. W. (1999). nacre encodes a zebrafish microphthalmia-related protein that regulates neural-crest-derived pigment cell fate. *Development* **126**, 3757-3767

Lister, J. A. (2002) Development of pigment cells in the zebrafish embryo. *Microsc. Res. Tech.* **58**, 435-441.

Lumsden, A., Sprawson, N. and Graham, A. (1991). Segmental origin and migration of neural crest cells in the hindbrain region of the chick embryo. *Development* **113**, 1281-1291.

Luo, R., An, M., Arduini, B. L. and Henion, P. D. (2001). Specific pan-neural crest expression of zebrafish Crestin throughout embryonic development. *Dev. Dyn.* **220**, 169-174.

Luo, T., Matsuo-Takasaki, M., Thomas, M. L., Weeks, D. L. and Sargent, T. D. (2002). Transcription factor AP-2 is an essential and direct regulator of epidermal development in Xenopus. *Dev. Biol.* **245**, 136-144.

Maconochie, M., Krishnamurthy, R., Nonchev, S., Meier, P., Manzanares, M., Mitchell, P. J. and Krumlauf, R. (1999). Regulation of *Hoxa2* in cranial neural crest cells involves members of the AP-2 family. *Development* **126**, 1483-1494.

Manie, S., Santoro, M., Fusco, A. and Billaud, M. (2001). The RET receptor:

function in development and dysfunction in congenital malformation. *Trends Genet.* **10**, 580-589.

Marusich, M. F., Furneaux, H. M., Henion, P. D. and Weston, J. A. (1994). Hu neuronal proteins are expressed in proliferating neurogenic cells. *J. Neurobiol.* **25**, 143-155.

Maschhoff, K. L. and Baldwin, H. S. (2000). Molecular determinants of neural crest migration. *Am. J. Med. Genet.* **97**, 280-288.

Meier, P., Koedood, M., Philipp, J., Fontana, A. and Mitchell, P. J. (1995). Alternative mRNAs encode multiple isoforms of transcription factor AP-2 during murine embryogenesis. *Dev. Biol.* **169**, 1-14.

Meulemans, D. and Bronner-Fraser, M. (2002). Amphioxus and lamprey AP-2 genes: implications for neural crest evolution and migration patterns. *Development* **129**, 4953-4962.

Miller, C. T., Schilling, T. F., Lee, K., Parker, J. and Kimmel, C. B. (2000). Sucker encodes a zebrafish *Endothelin-1* required for ventral pharyngeal arch development. *Development* **127**, 3815-3828.

Mitchell, P. J., Timmons, P. M., Hebert, J. M., Rigby, P. W. J. and Tijan, R. (1991). Transcription factor Ap-2 is expressed in neural crest cell lineages during mouse embryogenesis. *Genes Dev.* **5**, 105-119.

Morriss-Kay, G. M. (1996). Craniofacial defects in AP-2 null mutant mice. *BioEssays* **18**, 785-788.

Moser, M., Imhof, A., Pscherer, A., Bauer, R., Amselgruber, W., Sinowatz, F., Hofstadter, F., Schule, R. and Buettner, R. (1995). Cloning and characterization of a second AP-2 transcription factor: AP-2 beta. *Development* **121**, 2779-2788.

Moser, M., Ruschoff, J. and Buettner, R. (1997). Comparative analysis of AP-2 alpha and AP-2 beta expression during murine embryogenesis. *Dev. Dyn.* **208**, 115-124.

Nakata, K., Nagai, T., Aruga, J. and Mikoshiba, K. (1997). Xenopus *Zic3*, a primary regulator both in neural and neural crest development. *Proc. Natl. Acad. Sci. USA* **94**, 11980-11985.

Nakata, K., Nagai, T., Aruga, J. and Mikoshiba, K. (1998). Xenopus Zic family and its role in neural and neural crest development. *Mech. Dev.* **75**, 43-51.

Neave, B., Rodaway, A., Wilson, S. W., Patient, R. and Holder, N. (1995). Expression of zebrafish *gata 3* (*gta3*) during gastrulation and neurulation suggests a role in the specification of cell fate. *Mech. Dev.* **51**, 169-182.

Neuhauss, S. C., Solnica-Krezel, L., Schier, A. F., Zwartkruis, F., Stemple, D. L., Malicki, J., Abdelilah, S., Stainier, D. Y. and Driever, W. (1996). Mutations affecting craniofacial development in zebrafish. *Development* **123**, 357-367.

Nieto, M. A., Sargent, M. G., Wilkinson, D. G. and Cooke, J. (1994). Control of cell behavior during vertebrate development by *Slug*, a zinc finger gene. *Science* **264**, 835-839.

Nieto, M. A. (2001). The early steps of neural crest development. *Mech. Dev.* **105**, 27-35.

Nieto, M. A. (2002). The Snail superfamily of zinc-finger transcription factors. *Nat. Rev. Cell Mol. Biol.* **3**, 155-166.

Noden, D. M. (1983). The role of the neural crest in patterning of avian cranial skeletal, connective and muscle tissues. *Dev. Biol.* **96**, 144-165.

Nottoli, T., Hagopian-Donaldson, S., Zhang, J., Perkins, A. and Williams, T. (1998). AP-2-null cells disrupt morphogenesis of the eye, face and limbs in chimeric mice. *Proc. Natl. Acad. Sci. USA* **95**, 13714-13719.

Odenthal, J. and Nusslein-Volhard, C. (1998). Forkhead domain genes in zebrafish. *Dev. Genes Evol.* **208**, 245-258.

Parichy, D. M., Rawls, J. F., Pratt, S. J., Whitfield, T. T. and Johnson, S. L. (1999). Zebrafish *sparse* corresponds to an orthologue of *c-kit* and is required for the morphogenesis of a subpopulation of melanocytes, but is not essential for hematopoiesis or primordial germ cell development. *Development* **126**, 3425-3436.

Parichy, D. M., Ransom, D. G., Paw, B., Zon, L. I. and Johnson, S. L. (2000a). An orthologue of the kit-related gene *fms* is required for development of neural crest-derived xanthophores and a subpopulation of adult melanocytes in the zebrafish, Danio rerio. *Development* **127**, 3031-3044.

Parichy, D. M., Mellgren, E. M., Rawls, J. F., Lopes, S. S., Kelsh, R. N. and Johnson, S. L. (2000b). Mutational analysis of *endothelin receptor b1* (*rose*) during neural crest and pigment pattern development in the zebrafish (Danio rerio). *Dev. Biol.* **227**, 294-306.

Pelletier, I., Bally-Cuif, L. and Ziegler, I. (2001). Cloning and developmental expression of zebrafish GTP cyclohydrolase I. *Mech. Dev.* **109**, 99-103

Pfisterer, P., Ehlermann, J., Hegen, M. and Schorle, H. (2002). A subtractive gene expression screen suggests a role of transcription factor AP-2 alpha in control of proliferation and differentiation. *J. Biol. Chem.* **277**, 6637-6644.

Prince, V. and Lumsden, A. (1994). Hoxa-2 expression in normal and transposed rhombomeres: independent regulation in the neural tube and neural crest. *Development* **120**, 911-923.

Prince, V. E., Moens, C. B., Kimmel, C. B. and Ho, R. K. (1998). Zebrafish hox genes: expression in the hindbrain region of wild-type and mutants of the segmentation gene, *valentino*. *Development* **125**, 393-406.

Rijli, F. M., Mark, M., Lakkaraju, S., Dierich, A., Dolle, P. and Chambon, P. (1993). A homeotic transformation is generated in the rostral branchial region of the head by disruption of Hoxa-2, which acts as a selector gene. *Cell* **75**, 1333-1349.

Rubinstein, A. L., Lee, D., Luo, R., Henion, P. D. and Halpern, M. E. (2000). Genes dependent on zebrafish cyclops function identified by AFLP differential gene expression screen. *Genesis* **26**, 86-97.

Sasai, N., Mizuseki, K. and Sasai, Y. (2001). Requirement for FoxD3-class signaling for neural crest determination in Xenopus. *Development* **128**, 2525-2536.

Schilling, T. F. (1997). Genetic analysis of craniofacial development in the vertebrate embryo. *BioEssays* **19**, 459-468.

Schilling, T. F. and Kimmel, C. B. (1994). Segment and cell type lineage restrictions during pharyngeal arch development in the zebrafish embryo. *Development* **120**, 2945-2960.

Schilling, T. F., Walker, C. and Kimmel, C. B. (1996a). The *chinless* mutation and neural crest cell interactions during zebrafish jaw development. *Development* **122**, 1417-1426.

Schilling, T. F., Piotrowski, T., Grandel, H., Brand, M., Heisenberg, C.-P., Jiang, Y. J., Beuchle, D., Hammerschmidt, M., Kane, D. A., Mullins, M. et al. (1996b). Jaw and branchial arch mutants in zebrafish I: branchial arches. *Development* **123**, 329-344.

Schorle, H., Meier, P., Buchert, M., Jaenisch, R. and Mitchell, P. J. (1996). Transcription factor AP-2 essential for cranial closure and craniofacial development. *Nature* **381**, 235-238.

Sefton, M., Sanchez, S. and Nieto, M. A. (1998). Conserved and divergent roles for members of the Snail family of transcription factors in the chick and mouse embryo. *Development* **125**, 3111-3121.

Shimeld, S. M. and Holland, P. W. H. (2000). Vertebrate innovations. *Proc. Natl. Acad. Sci. USA* **97**, 4449-4452.

Soo, K., O-Rourke, M. P., Khoo, P. L., Steiner, K. A., Wong, N., Behringer, R. R. and Tam, P. P. (2002). Twist function is required for the morphogenesis of the neural tube and the differentiation of the cranial neural crest cells in the mouse embryo. *Dev. Biol.* **247**, 251-270.

Stachel, S. E., Grunwald, D. J. and Myers, P. Z. (1993). Lithium perturbation and *goosecoid* expression identify a dorsal specification pathway in the pregastrula zebrafish. *Development* **117**, 1261-1274.

Tassabehji, M., Read, A. P., Newton, V. E., Patton, M., Gruss, P., Harris, R. and Strachan, T. (1993). Mutations in the *PAX3* gene causing Waardenburg syndrome type 1 and type 2. *Nat. Genet.* **3**, 26-30.

Thisse, C., Thisse, B., Schilling, T. F. and Postlethwait, J. H. (1993). Structure of the zebrafish *snail1* gene and its expression in wild-type, *spadetail* and *no tail* mutant embryos. *Development* **119**, 1203-1215.

Thisse, C., Thisse, B. and Postlethwait, J. H. (1995). Expression of *snail2*, a second member of the zebrafish snail family, in cephalic mesendoderm and presumptive neural crest of wild-type and *spadetail* mutant embryos. *Dev. Biol.* **172**, 88-96.

Tumpel, S., Maconochie, M., Wiedemann, L. M. and Krumlauf, R. (2002). Conservation and diversity in the cis-regulatory networks that integrate information controlling expression of Hoxa2 in hindbrain and cranial neural crest cells in vertebrates. *Dev. Biol.* **246**, 45-56.

Werling, U. and Schorle, H. (2002). Transcription factor gene AP-2 gamma essential for early murine development. *Mol. Cell. Biol.* **22**, 3149-3156.

Williams, T. and Tjian, R. (1991). Analysis of the DNA-binding and activation properties of the human transcription factor AP-2. *Genes Dev.* **5**, 670-682.

Zhang, J. A., Hagopian-Donaldson, S., Serbedzija, G., Elsemore, J., Plehn-Dujowich, D., McMahon, A. P., Flavell, R. A. and Williams, T. (1996). Neural tube, skeletal and body wall defects in mice lacking transcription factor AP-2. *Nature* **381**, 238-241.